An analysis of the robustness of the RVT Correction in the presence of Non-white noise processes in fMRI Data

E. B. Beall[1], and M. J. Lowe[1]

[1]Radiology, Cleveland Clinic, Cleveland, OH, United States

Introduction

Variations in breathing rate and depth have been shown to produce significant effects on the BOLD-weighted fMRI signal throughout gray matter[1-3]. These effects are present globally with low frequencies, within the range of frequencies of low-frequency BOLD fluctuations (LFBF), or functional connectivity. As a result, variations in respiration may be a confound in the analysis of resting-state fMRI data. A recent study proposed to account for this effect by monitoring subject breathing during resting fMRI scans and then regressing respiratory variation from the voxel timeseries[3]. That study observed coupling to breathing variation in the posterior cingulate and other regions of what has been termed the "default mode network". This network of synchronized fMRI signal, as well as other synchronized networks post-hoc identified as potentially functionally relevant, is characterized by the LFBF of functional connectivity, which several recent studies have used as support in their characterization of those networks as functionally relevant[4]. The method proposed by Birn et al. creates a signal characterizing respiratory varation over time (RVT) by multiplying respiratory volume by respiratory rate to approximate total intake of fresh air. Increases in this signal are expected to result in decreases in end-tidal CO_2 and by its action as a vasodilator, decrease the fMRI signal. It is expected to take several seconds for this action to occur, due to a lag in perfusion from lungs to head and a lag in arterial capillary bed response to changed CO_2 level. To account for this lag, the method performs a phase search over temporal shifts of RVT for every voxel timeseries and uses the phase shifted RVT timecourse with greatest negative correlation as the regressor. However, due to the low frequency of the RVT signal, the false positive rate from the search process can be expected to dramatically increase in regions containing high LFBF power. Therefore it is possible the phase search portion of the RVT correction produces incorrect lags in those regions. We perform a simulation study to show the lag search can fail in the presence of LFBF and show a range of lags detected in real fMRI data by the RVT algorithm.

Methods

The following three scans were performed on sixteen subjects. Scan1: anatomic whole-brain T1-weighted inversion recovery turboflash (MPRAGE), 120 axial slices, thickness 1.2mm, Field-of-view (FOV) 256mm×256mm, matrix=256×128. Scans 2-3: whole-brain EPI scans: 132 volumes of 31-4mm thick axial slices TE/TR/flip = 29ms/2000ms/90°, matrix=64×64, 256mm ×256mm FOV, BW=125KHz. Physiologic data is measured in parallel for the EPI scans with a finger pulse plethysmograph and a respiratory bellows around the chest. The respiratory bellows data is postprocessed to produce the RVT estimator[3]. These two fMRI datasets were passed to the RVT correction.

Simulation

The following eight sources were injected at each voxel: five functionally relevant spatial network sources characterized by LFBF, two physiologic noise sources (parallel measured pulse and chest expansion data measured in real subjects) and an RVT noise source. The spatial distribution of the power of functional sources were determined as follows: each of 16 subjects' resting state fMRI scans were spatially normalized, detrended and variance normalized, concatenated in the temporal dimension and passed to spatial ICA. Following ICA decomposition, spatial networks that were similar to those described by others [4] were identified. The spatial vectors for these sources were then saved for the purpose of injecting low frequency noise in the range of LFBF into the simulation. Physiologic spatial weight vectors were determined using PESTICA[5]. Using the same data, the SNR of the first seven sources were determined by regressing known sources of interest (five spatial ICA-determined timecourses relating to the five functional spatial networks and the parallel measured pulse and respiration for the physiologic regressors using the algorithm of RETROICOR [6]) and producing a mean and standard deviation of the fit coefficients for use in the simulation. However, RVT regression is hypothesized to be problematic, so we could not use regression to determine the approximate SNR. Therefore, the SNR was varied over a range below and approaching that of the other physiologic sources. Finally, the spatial distribution of RVT noise was created randomly, so as to minimize intentional overlap with the other sources. The lag for each simulation was chosen from a uniform random distribution ranging from 4 to 8 seconds. The injected sources, maps and lag chosen were saved for each simulation for comparison with the final fit maps. An SNR level of 50 relates to a percent signal variation level of 2.5%. 32 datasets are created for each SNR level and passed to the RVT correction, which was performed using the injected pulse and respiration data and the RVT estimator injected in the simulation. At each SNR level, the lags detected for each voxel are histogrammed, and this histogram is averaged across the 32 simulated datasets, giving an average lag curve for each SNR level.

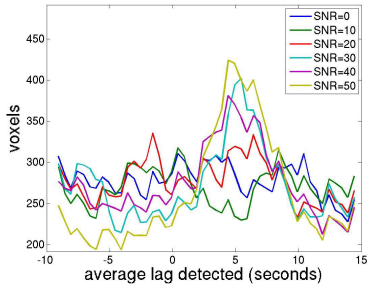

Fig 1: histogram of RVT lags detected in simulation at various levels of injected RVT SNR. Injected lag ranges from 4-8 seconds.

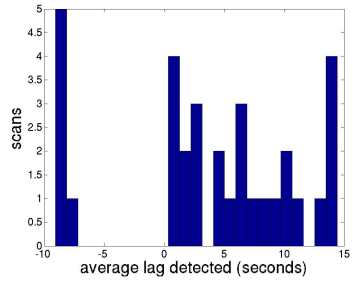

Fig 2: histogram of RVT lags detected in 32 fMRI datasets.

RVT Correction

This estimator and the respiratory and pulse data are passed to the RVT correction, which is a modified form of the RETROICOR algorithm. RVT correction performs a voxelwise regression of pulse, respiration and various phase-lagged RVT estimates and searches for the most negative fit of RVT to the voxel timecourse (minimum is used since increases in RVT lead to decreases in fMRI signal, like the effect of a breath-hold increasing global fMRI signal). This phase searching is performed separately at each voxel, and the final lag and fit coefficient at each voxel is saved. The raw data is passed to this algorithm and the average lag detected in every voxel is histogrammed, and the maximum histogram bin is selected as the lag detected. This lag is histogrammed for the 32 fMRI datasets available.

Results

The averaged histogrammed lags detected in the simulated datasets by the phase-searching procedure are shown in Fig 1. Six levels of SNR are shown, and for SNR levels less than 30, there is no clear peak near the injected lag around 6 seconds. At and above this SNR, the average lag detected is near the injected lag. However, even at an SNR of 50, over 50% of lags detected are not within the 4-8 second range of the injected lags. In real data, the situation is similar, with the average of lags detected giving a curve similar to the simulation curve with SNR=40. The maximum lag detected is histogrammed for the 32 fMRI datasets in Fig 2. Note that about 20% are negative and the rest spread from 0 to 15 seconds.

Discussion and Conclusion

Based on the simulation study, we can state that, due to the delay search process, the RVT correction is sensitive to the strength of the artifactual presence in the data. Even for a fairly strong RVT effect similar to that observed by others [3], over half of voxels will end up with the wrong lag used in the regression. It is likely that, in the presence of strong LFBF signal, the delay is incorrectly identified and the result could be detrimental to the detection of LFBF effects after the correction. The distribution of lags observed in the human data was similar to that observed in the simulations, suggesting that the SNR of the RVT effect is not strong enough for the delay search process to be robust. Also, the average lag detected in most cases does not correspond to that expected by the primary hypothesized physical model of RVT; that RVT correlates with end-tidal CO_2. A possible modification to the RVT algorithm may be to explicitly include ICA-derived functional network timecourses as covariates in the phase-searching regression and finally fixing the lag used in the regression to the global lag detected.

References

1). Kastrup et al, 1999 Magn. Reson. Med., 42(3): 608-611, 2). Wise et al, 2004 NeuroImage, 21(4): 1652-1664, 3). Birn et al, 2006 NeuroImage, 31(4): 1536-1548, 4). Beckmann et al, 2004 IEEE Trans Med Imaging 23, 137-152, 5). Beall and Lowe, 2007 NeuroImage, 37(4): 1286-1300, 6). Glover et al, 2000 Magn. Reson. Med. 44, 162-167